MECHANICS OF A CYLINDRICAL FLEXIBLE WEB FLOATING OVER AN AIR-REVERSER

by

S. Müftü[1] and K. A. Cole[2]
[1]Massachusetts Institute of Technology
[2]Eastman Kodak Company
USA

ABSTRACT

The mechanics of the fluid/structure interaction between a thin flexible web, wrapped around a cylindrical drum (reverser), and the air cushion formed by external pressurization through the holes of this drum is analyzed. The web deflections are modeled by a cylindrical shell theory that allows moderately large deflections. The airflow is modeled in two-dimensions with a modified form of the Navier-Stokes and mass balance equations, with non-linear source terms. The coupled fluid/structure system is solved numerically. The mechanics of the interaction between the web deflections and the air cushion generated by the reverser is explained. The effects of the problem parameters on the overall equilibrium are presented.

NOMENCLATURE

b	$(D/T)^{1/2}$	α	Density of hole distribution
c	Web thickness	ρ	Density of air
D	Bending stiffness of the web	μ	Viscosity of air
D_s	Shell stiffness of the web	κ	Discharge coef. at holes
E	Young's Modulus of the web	κ_b	Discharge coef. on the periphery
h	Web-reverser clearance	λ	1/4
L_1, L_2	Locations of the tangency points	$\tau_{z^*x^*}$, $\tau_{z^*y^*}$	Wall shear stress in the fluid
L_x, L_y	The length and width of the web	θ	$\arctan(v^*/u^*)$
p	Air pressure in the clearance	ν	Poisson's ratio
p_0	Supply pressure in the reverser	δ	Function used in defining web reverser spacing
$R(x)$	Web radius at final state		
$R_0(x)$	Web radius at *initial-ref.* state	δ_L, δ_R	The left and right side definitions of δ
T	Web tension	$\nabla^4(\,)$	The bi-harmonic operator: $(\,)_{,xxxx} + 2(\,)_{,xxyy} + (\,)_{,yyyy}$
u^*, v^*	Airflow speeds in x* and y* dirs.		
U	Airflow speed out of a hole		
U_0	$(2p_0/\rho)^{1/2}$		

x, y Coordinate axes on the web
x^*, y^* Coordinate axes for the reverser
w Final web deflection
w_r *Self-adjusting reference state*
w_0 *Initial-state* of the web

INTRODUCTION

An air-reverser is a hollow, cylindrical, porous drum used in web handling applications where it is important to change the direction of a web without contact. The web floats over an air cushion formed in the web-reverser clearance, by injecting air through the holes of the reverser. Thus the web direction can be changed without contacting the underlying drum. Figure 1 shows a web floating over a reverser. A typical web path is equipped with an active tension control mechanism that keeps the web tension constant. Therefore, relatively large web deflections can be implemented without inducing large strains. The steady state air pressure in the interface is inversely related to the web-reverser clearance h (1)[1]. Therefore, while the air injected into the clearance causes the web to deflect away from its initial state, increasing clearance causes reduction of the air pressure. Thus the fluid mechanics of air is coupled to the deflection of the web and vice versa. The coupled system eventually settles to a steady-state clearance.

A problem similar to the fluid/structure interaction of the air-reverser is encountered in externally pressurized foil bearings (2). However, the viscous forces dominate the airflow in the narrow clearance of the foil-bearing problem, whereas in the air reverser problem airflow is dominated by the inertial forces (1). Viscous flow constitutes a relatively small fraction (10-20%) of the average air pressure in the clearance (3).

The two-dimensional air-reverser flow model of Lewis uses averaged values of air velocities u^* and v^*, and air pressure p in the clearance height direction: the governing equations of the flow are a modified form of the incompressible Navier-Stokes and mass balance equations with non-linear source terms (1,3). This model is used in this paper. The interaction of a single Coanda jet with a flexible flat web has been studied by Quadracci and Modi (4), where the web is assumed to be infinitely wide. The main fluid mechanical effect in this case is the creation of a reliable source of air-suction to stabilize the web. An experimental study on this subject has been reported by Pimenov and Galimov (5).

In this paper, web deflections are modeled by a moderately large deflection "cylindrical" shell theory with a continuous curvature variation and a *self-adjusting reference state*, near the steady state of the web (6). This new approach creates an efficient method in representing the deflection history of the web, arising from its initial wrapping around the drum and its subsequent motions to keep a nearly constant tension level. The governing equations are based on an extension of Donnell's (7) theory on cylindrical shells. Lin and Mote (8) used the von Karman plate theory to study the buckling of a flat web in the free span between two rollers. The subject of wrapping a thin web around a cylindrical drum, over large wrap-angles was treated in references (9-12). In the present work, a continuous function for the curvature variation of a relatively

[1] The numbers in parenthesis refer to the references given at the end of the paper.

thick web, wrapped around a cylindrical drum, is used. The continuous web curvature, as it will be defined here, has also been treated in references (6,13).

A self-adjusting reference state in connection with the analysis of flexible tapes was first described by Barlow (14). The in-plane stresses were referred to a self-adjusting cylindrical surface as described here, but the bending moments were described with respect to the undeflected configuration w_o in contrast to the present work. The equations were, then, reduced to an infinitely wide web where the effects vanish. The adjustable reference radius was used in (15), where the radial deflections of a cylindrical shell wrapped around a bumpy drum is analyzed for the circumferentially symmetrical case.

GOVERNING EQUATIONS

Web Deflection Equations

The equations governing the web deflections are given by Müftü and Cole (6),

$$D\nabla^4 \bar{w} + D_s \bar{w} - T\frac{\partial^2 w}{\partial x^2} = p - \frac{T}{R(x)} \qquad \{1\}$$

$$\text{with } \bar{w} = w - w_r$$

where D is the bending stiffness, D_s is the shell stiffness, $R(x)$ is the radius of curvature, and T is the longitudinal tension of the web, p is the air pressure, and $T/R(x)$ is the pull-down pressure. In equation {1}, $\bar{w}$ represents the actual web deflection measured with respect to the *initial-reference state*, w_0, and w, represents the web deflections which cause the bending moments and in-plane stretching. The latter deflection is measured from the *self-adjusting reference state*, w_r, which is defined by the cylindrical surface extending laterally from the mid-line of the steady state of the web deformation, as shown in Figure 1. This reference state is employed in order to model large web deflections, while the strains are moderately large (6). The bending and shell stiffness of the web are defined as,

$$D = \frac{Ec^3}{12(1-\nu^2)} \quad \text{and} \quad D_s = \frac{Ec}{R^2(x)(1-\nu^2)} \qquad \{2\}$$

where E is the elastic modulus, ν is the Poisson's ratio, and c is the thickness of the web. The radius of curvature of the web varies along the longitudinal direction x. At the *initial-reference state*, w_0, shown in Figure 1, the radius of curvature of the web, $R_0(x)$, is,

$$\frac{1}{R_0(x)} = \frac{1}{R_c}\begin{cases} \exp\left[-\left(1+\dfrac{L_1-x}{b}\right)\right], & \text{for } 0 \le x \le L_1 + b, \\ 1, & \text{for } L_1 + b \le x \le L_2 - b, \\ \exp\left[-\left(1+\dfrac{x-L_2}{b}\right)\right], & \text{for } L_2 - b \le x \le L_x, \end{cases} \qquad \{3\}$$

where $b = (D/T)^{1/2}$ is the characteristic bending length of the web (6). Note that, $R(x)$ at the actual web deflection is obtained from $R(x) = R_0(x)+w$. For a typical air reverser application, w is much smaller than $R_0(x)$, therefore, in this paper it is assumed that $R(x) \cong R_0(x)$. The boundary conditions for the web deformations are,

$$\text{At } x = 0, L_x, \text{ and } 0 \le y \le L_y : D\left(\frac{\partial^2 \overline{w}}{\partial x^2} + \nu \frac{\partial^2 \overline{w}}{\partial y^2}\right) = 0, \qquad \{4\}$$
$$\overline{w} = 0,$$

$$\text{At } y = 0, L_y, \text{ and } 0 \le x \le Lx : D\left(\frac{\partial^2 \overline{w}}{\partial y^2} + \nu \frac{\partial^2 \overline{w}}{\partial x^2}\right) = 0, \qquad \{5\}$$
$$D\left(\frac{\partial^3 \overline{w}}{\partial y^3} + (2-\nu)\frac{\partial^3 \overline{w}}{\partial x^2 \partial y}\right) = 0,$$

The clearance h between the web and the reverser, at a given location (x,y) on the web, is measured along the normal to the surface of the reverser, as shown in Figure 1. This is represented mathematically as,

$$h(x, y) = w(x, y) + \delta(x),$$

$$\text{where} \delta(x) = \begin{cases} \delta_L, \text{left flat - region,} \\ 0, \text{wrap - region,} \\ \delta_R, \text{right flat - region,} \end{cases} \qquad \{6\}$$

where $\delta_L(x)$ and $\delta_R(x)$ represent the clearance between the *initial reference state* of web and the reverser, on the flat region of the web. Figure 2 gives the $\delta(x)$ distribution used for the cases analyzed in this paper. Note that the function $\delta(x)$ remains constant throughout the solution process.

Fluid Mechanics of the Air-Reverser

In a typical application, the web-reverser clearance h is smaller than the other dimensions of the problem. Thus, the flow velocities u^* and v^*, parallel to the reverser surface, and the air pressure p can be averaged in the normal direction, and the flow velocity in the direction normal to the reverser surface w^* can be neglected. The hole distribution over the surface of the reverser is averaged locally (1). This average is indicated by α.

The governing equations for the steady state airflow in the web-reverser clearance then become the modified mass-continuity and Navier-Stokes equations given by Müftü et al. (3). These equations are expressed in a Cartesian coordinate frame (x^*,y^*) located on the reverser surface as,

$$\frac{\partial hu^*}{\partial x^*}+\frac{\partial hv^*}{\partial y^*}=\alpha U$$

$$\rho\left(u^*\frac{\partial u^*}{\partial x^*}+v^*\frac{\partial u^*}{\partial y^*}\right)=-\frac{\partial p}{\partial x^*}+\mu\left(\frac{4}{3}\frac{\partial^2 u^*}{\partial x^{*2}}+\frac{\partial^2 u^*}{\partial y^{*2}}+\frac{1}{3}\frac{\partial^2 v^*}{\partial x^*\partial y^*}\right)$$
$$-2\frac{\tau_{z^*x^*}}{h}-\alpha\rho U\frac{u^*}{h} \qquad \{7\}$$

$$\rho\left(u^*\frac{\partial v^*}{\partial x^*}+v^*\frac{\partial v^*}{\partial y^*}\right)=-\frac{\partial p}{\partial y^*}+\mu\left(\frac{4}{3}\frac{\partial^2 v^*}{\partial y^{*2}}+\frac{\partial^2 v^*}{\partial x^{*2}}+\frac{1}{3}\frac{\partial^2 u^*}{\partial x^*\partial y^*}\right)$$
$$-2\frac{\tau_{z^*y^*}}{h}-\alpha\rho U\frac{v^*}{h}$$

where ρ is the density, μ is viscosity of air and U is the air velocity through the reverser holes. The web-reverser clearance h is measured along a normal to the reverser surface. The wall-shear stresses $\tau_{z^*x^*}$ and $\tau_{z^*y^*}$, which occur at the web and reverser surfaces, are estimated from the 1/7-th-power-velocity distribution law (16) for the case of turbulent flow in a two-dimensional channel,

$$\tau_{z^*x^*}=\frac{1}{2}\rho 0.0676\cos\theta\left(\frac{\rho h}{\mu}\right)^{\lambda}\left(u^{*2}+v^{*2}\right)^{(2-\lambda)/2}$$
$$\tau_{z^*x^*}=\frac{1}{2}\rho 0.0676\sin\theta\left(\frac{\rho h}{\mu}\right)^{\lambda}\left(u^{*2}+v^{*2}\right)^{(2-\lambda)/2} \qquad \{8\}$$

where $\theta=\arctan(v^*/u^*)$ and $\lambda=1/4$ (3). The air velocity through the holes U depends on the pressure drop between the supply pressure p_0 inside the reverser and the local air pressure in the clearance. This velocity is expressed as,

$$U=\kappa U_0(1-p/p_0)^{1/2} \qquad \{9\}$$

where $U_0=(2p_0/\rho)^{1/2}$ and $\kappa \subset [0,1]$ is an empirically determined discharge coefficient, which represents the frictional losses at the exit of the holes. The effect of the momentum of the incoming air near the holes is only approximately included by this method. However, the overall momentum balance should be preserved if the correct value of κ can be found. Experiments show that for the reversers of interest, κ varies between 0.65 and 0.9 (3). A value of $\kappa=1$ was used in this paper.

On the outer periphery of the web-reverser clearance the air velocity is substantially high. Therefore, the following exit boundary condition for the air pressure is prescribed,

$$p=P_a-\frac{1}{2}\rho\kappa_b\left(u^{*2}+v^{*2}\right) \text{ on the boundary,} \qquad \{10\}$$

where κ_b is a discharge coefficient for the exit flow at the boundary and $P_a=0$ is the ambient pressure. A value of $\kappa_b=1$ was used in this paper. No exit conditions for the

flow is necessary. The governing equations are solved numerical as described in references (6,17).

RESULTS

The mechanics of a flexible cylindrical web and the air cushion generated by an air-reverser is investigated in this section. The physical parameters of the cases are given in Table 1. In particular, we present the effect of hole density distribution α, supply pressure p_0 and web tension T on the steady state web deflection. The web tension in these tests is T = 125 N/m and the reverser radius is R_c = 0.25 m. Thus the pull down pressure in the wrap-region is T/R = 500 Pa. Supply pressure is changed in the range $1 < p_0R/T \leq 3$.

The Effect of Hole Distribution on Steady State

Figure 3 shows the four different hole density distributions, case-1-4, tested numerically in this paper. In particular, cases shown in Figures 3.a and 3.d have holes distributed uniformly on the entry and exit sides of the reverser with $\alpha_1 = 0.025$ and $\alpha_4 = 0.1$, respectively. Case-2 has holes distributed uniformly around the outer periphery of the reverser with $\alpha_2 = 0.025$, and Case-3 has a variable hole density distribution with α_3 having values 0.025 and 0.1 on different parts of the entry and exit sides.

The air pressure and velocity distributions at steady state, for the supply pressure p_0 = 600 Pa, are shown in Figure 4. This figure shows that, in general, a slow moving air layer exists in the central part of the clearance, where the air pressure attains high values. The velocity of air increases toward the outer periphery and the air pressure decreases accordingly. Note that the air velocity and pressure distributions are "symmetrical" in these tests, since the shear coupling between the web and the reverser is neglected.

In case-1, which has the lowest hole density, the central high-pressure region is confined to a relatively small area in the center of the clearance; the air leaves from the lateral edges at high velocities. In contrast, in case-2, air coming from the lateral holes acts as a pressure wall and more air is confined in the central region. As a result the air pressure is higher in a larger part of the central region and the air exit velocity around the periphery is more uniform. This was also discussed in reference (1). In case-3 and case-4, where no lateral holes exist, the pressure and airflow distributions are, in general, similar to case-1. However, as the hole densities for these two cases are higher, the high-pressure regions extend toward the left and right edges as compared to case-1.

The corresponding web deflections, w, are presented in Figure 5. In this figure, the web deflections are measured with respect to the initial state of the web w_0. In general, Figure 5 shows that the web deflection in the wrap-region is distinctly different than in the no-wrap region: In the wrap-region, the web remains relatively flat in the lateral direction, where as in the no-wrap region the web has considerable relative deflection on its lateral edges. This difference in web deflection is due to the in-plane stiffness of the web in the wrap-region, and lack thereof in the no-wrap region.

The steady state conditions are presented in more detail in Figure 6, where deflection and pressure cross-sections are given along the centerlines $(x,L_y/2)$ and $(L_x/2,y)$. The cross-section in the circumferential direction x shows that in case-3 and case-4, where more air is injected into the no-wrap region, the air pressure becomes considerably higher in this region, as compared to cases-1 and –2. Consequently, the web deflects more. This shows that the web deflection in the circumferential direction is strongly affected by the hole-density in the no-wrap region.

Figure 6 also gives the web deflection in the transverse direction y, *relative* to the lateral edge of the web. This figure shows that very small deflections take place in the transverse direction of the wrap-region, as compared to the circumferential direction; For case-1, case-3 and case-4 the maximum lateral deflection of the web is approximately 0.042 mm; For case-2, where there are pressure holes on the lateral edges, the maximum web deflection is approximately 0.095mm. This figure shows that the lateral deflection of the web closely follows the pressure profile under the web.

The Effect of Supply Pressure p_0 on Steady State

The effects of different supply pressures on the web-reverser clearance and on the air pressure distribution along the centerline of the web are shown in Figure 7. This figure shows that in general, increasing the supply pressure has the effect of increasing the web-reverser clearance. Here it can also be seen that in the wrap-region, increasing supply pressure does not cause appreciable pressure build-up. In the no-wrap region, modest air pressure increase is observed for case-1 and case-2, and significant pressure built-up is observed for case-3 and case-4.

These results indicate that, in the wrap-region, the air pressure balances the pull-down pressure on the web, T/R: Increasing supply pressure does not cause appreciable pressure built-up. On the other hand, in the no-wrap region significantly more pressure build-up occurs, as there is no external load on the web.

The effect of the supply pressure on the web-reverser clearance can be summarized by plotting the mid-point web-reverser clearance $h_{mid} = h(L_x/2,L_y/2)$ and the minimum web-reverser clearance h_{min} as a function of the normalized supply pressure p_0R/T as given in Figure 8. The plot of h_{mid}-vs-p_0R/T shows modest increase of h_{mid} for cases-1 and –2 as compared to cases-3 and –4. These figures also show that choosing the supply pressure in accordance to the relation $p_0 = T/R$ does not necessarily mean that possibility of contact would be prevented. In fact, for the hypothetical reversers modeled by cases-1 and –2, when $p_0R/T = 1.5$, the minimum web-reverser clearance value is predicted to be $h_{min} = 3$ mm. This may be on the lower limit of acceptability for practical applications.

The Effect of Web Tension on Steady State

The effect of web tension on the steady state conditions is tested numerically for two different tension values, $T = 59$ and $T = 236$ N/m. In these tests the normalized supply pressure p_0R/T is kept constant. Figure 9 shows the mid-cross-sections of the web deflections and air pressure in the circumferential and transverse directions of the web. It is interesting to note in this figure that the pressure profiles in both directions are very

nearly identical for both tensions. This is a good indication that the air pressure distribution in the clearance scales with normalized supply pressure p_0R/T. In the circumferential direction, the web deflections show small but noticeable variations. In the transverse direction the web with the higher tension deflects more than the web subject to lower tension.

SUMMARY AND CONCLUSIONS

The mechanics of the fluid/structure interaction between a flexible web and the air cushion generated by an air reverser is investigated by modeling. The effects of pressure hole density distribution supply pressure and web tension on the steady state conditions are studied. The following conclusions are reached:

- The equilibrium of the coupled web-reverser system works in such a way that; In the wrap-region, the pull-down pressure on the web, T/R, is balanced by the air pressure, and; In the no-wrap region, significantly more pressure build-up occurs, as there is no external load on the web.
- The web deflection in the circumferential direction is strongly affected by the hole-density in the no-wrap region. But, the shape of the web does not necessarily take the shape of the pressure profile. On the other hand, the shape of the transverse web deflection, in the wrap-region, matches closely the shape of the pressure profile.
- The shell stiffness in the wrap-region keeps the web from attaining large relative deflections in the transverse direction, whereas the opposite is true in the no-wrap region.
- At steady state, the stagnant air in the center region of the web provides support for the pull down pressure. The velocity of air increases toward the outer periphery and the air pressure decreases accordingly.
- Increasing the supply pressure has the effect of increasing the web-reverser clearance.
- In choosing the supply pressure, for the reverser cases-1 and -2 modeled here, the ratio p_0R/T should be greater than 1.5, in order to ensure an acceptable minimum web-reverser clearance.
- Using different tensions while keeping the p_0R/T constant has a small effect on the overall steady state conditions.

ACKNOWLEDGEMENTS

The first author gratefully acknowledges the support provided by the Eastman Kodak Company and the National Science Foundation through grant ECS-9615027.

REFERENCES

1. Müftü, S., Lewis T.S., Cole K.A. and Benson R.C., "Modelling of Fluid Dynamics of Air Reversers," ASME Journal of Applied Mechanics, Vol. 65, 1998, pp. 171-177.

2. Gross, W.A., ed. Fluid Film Lubrication, John Wiley & Sons, New York, 1980.

3. Müftü, S., Lewis T.S., Czuprynski, D.M. and Cole K.A. "A Simple Two Dimensional Model For Incompressible, Viscous Fluid Flow In An Externally

Pressurized Narrow Channel," 1998, Internal report, M.I.T. Haystack Observatory, Westford, MA.

4. Quadracci, H.R. and Modi, V., "Heat Transfer Of An Inclined Coanda Jet To A Flexible Web," ASME Paper 94-WA/HT-21, 1994.

5. Pimenov, V.G. and Galimov, M.M., "Use Of Air Blankets For The Drying And Transport Of Film Materials," Chemical and Petroleum Engineering, Vol. 30, No. 9-10, 1994, pp. 486-488, (Translated from Khimicheskoe i Neftyanoe Mashinostronie, No. 10, 18-20, Oct. 1994.)

6. Müftü, S. and Cole, K.A. "The Fluid/Structure Interaction in Supporting a Thin Flexible Cylindrical Web with an Air Cushion," in review Journal of Fluids and Structures, 1999.

7. Donnell, L.H., Beams, Plates and Shells, McGraw-Hill, New York, 1976.

8. Lin C.C. and Mote, Jr., C.D., "The Wrinkling Of Thin, Flat, Rectangular Webs," ASME Journal of Applied Mechanics Vol. 63, 1996, pp. 774-779.

9. Rongen, P.M.J., Finite Element Analysis of the Tape Scanner Interface in Helical Scan Recording, Ph.D. Dissertation, Technical University of Eindhoven, The Netherlands, 1994.

10. Sundaram, R. and Benson, R.C., "A Green's Function With Improved Convergence For Cylindrically Wrapped Tapes," Tribology and Mechanics of Magnetic Recording Systems, Society of Tribologists and Lubrication Engineers, Special Publication, Vol SP-16., 1989.

11. Müftü, S. and Benson R.C., "A Study Of Cross-Width Variations In The Two Dimensional Foil Bearing Problem," ASME Journal of Tribology Vol. 118, 1995, pp. 407-414.

12. Ono, K. and Ebihara, T., "Improved Green's Function In Tape Deflection And Solutions Of Head Contour With Uniform Contact Pressure," Tribology and Mechanics of Magnetic Recording Systems, Society of Tribologists and Lubrication Engineers, Special Publication, Vol. SP-16, 1984, pp. 97-102.

13. Benson, R.C., "Stiff Elastic Tape Wrapped Onto A Drum," ASME Journal of Applied Mechanics, Vol. 65, 1998, pp. 870-874.

14. Barlow, E. J., "Derivation Of Governing Equations For Self Acting Foil Bearing," *ASME Journal of Lubrication Technology*, July, 1967, pp. 334-340.

15. Benson R.C. and D'Errico, J.R. "The Deflection Of An Elastic Web Wrapped Around A Surface Of Revolution," Mechanics of Structures & Machines Vol. 19, pp. 467-486.

16. Schlicting, H., Boundary-Layer Theory, McGraw-Hill, New York, 1987.

17. Müftü, S., Lewis T.S. and Cole K.A., "A Numerical Solution Of The Euler's Equations With Nonlinear Source Terms In Modelling The Fluid Dynamics Of An Air Reverser," Proceedings of Information Storage and Processing Systems Symposium, ASME-IMECE, Dallas, TX, Vol. ISPS-3, 1997, pp. 39-48.

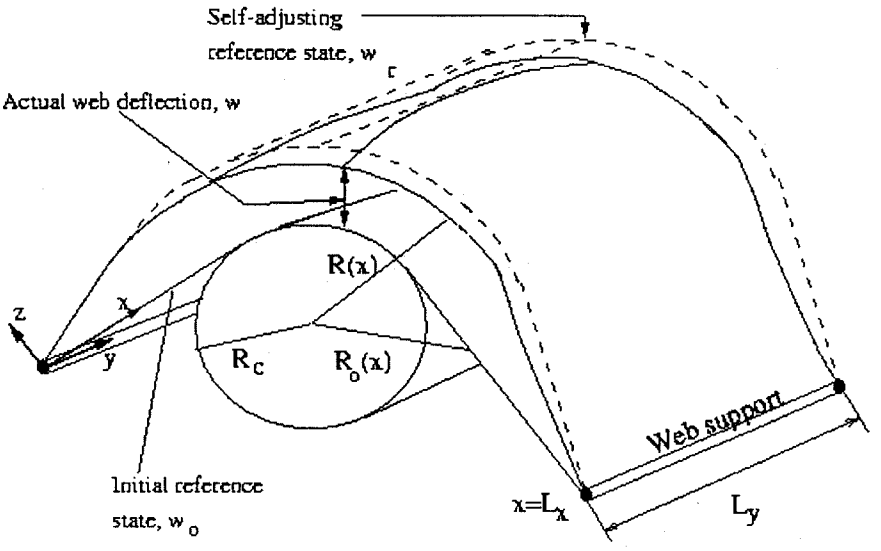

Figure 1 Schematic description of the initial-state, w_0, self-adjusting reference state, w_r and actual web deflection w. The function $\delta(x)$ used in describing the web-reverser clearance is also shown.

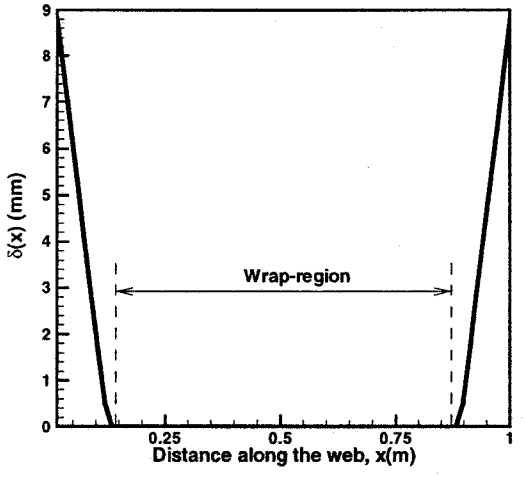

Figure 2 The function $\delta(x)$ used in cases presented in this paper, for calculating $h=w+\delta$.

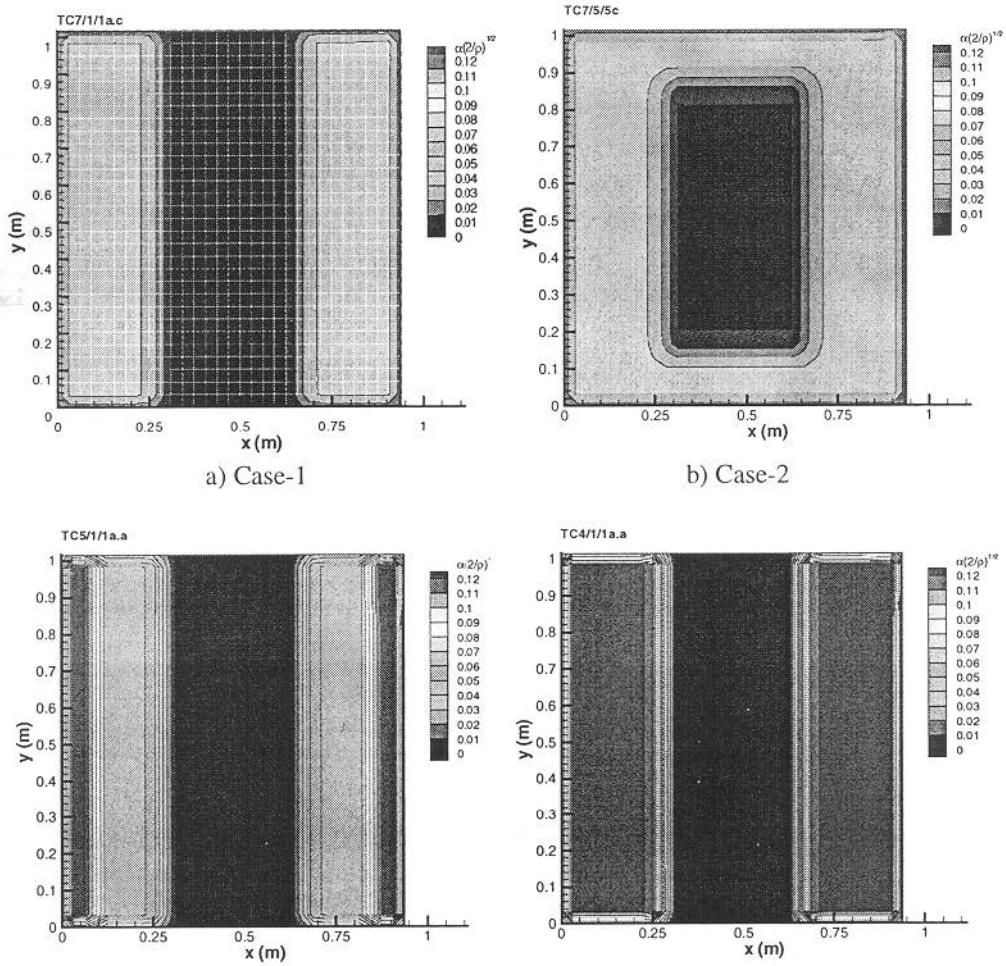

a) Case-1 b) Case-2

c) Case-3 d) Case-4

Figure 3 Hole density distribution α over the reverser surface. Note that air density ρ = 1.2 kg/m^3.

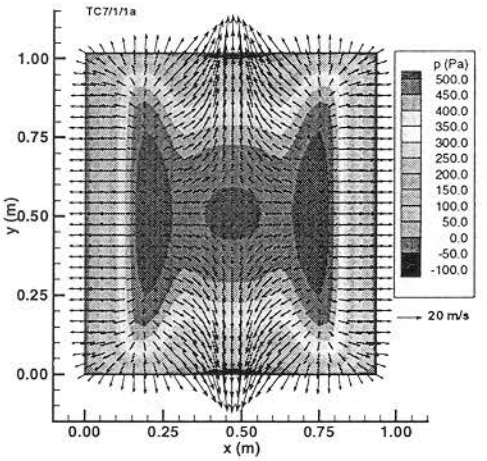

a) Case-1

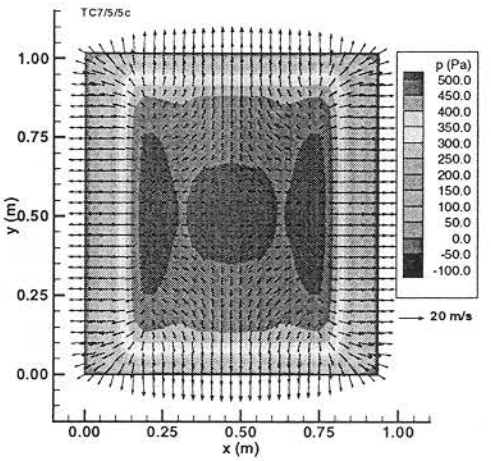

b) case-2

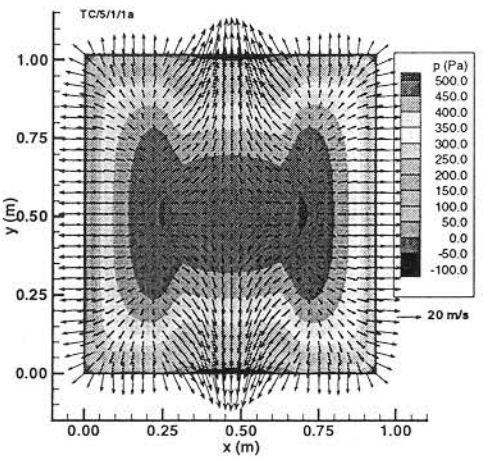

c) Case-3

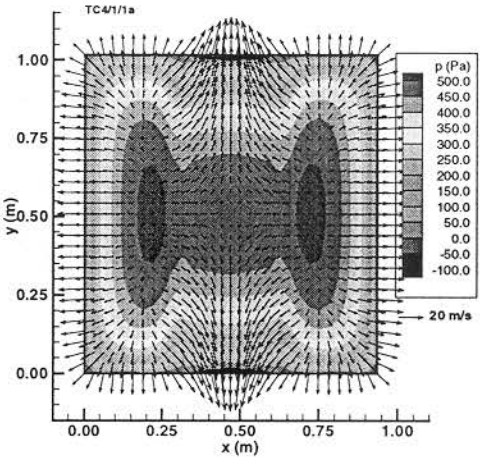

d) Case-4

Figure 4 This figure shows the air pressure and velocity distributions at steady state for cases-1-4, $p_0 = 600$ Pa.

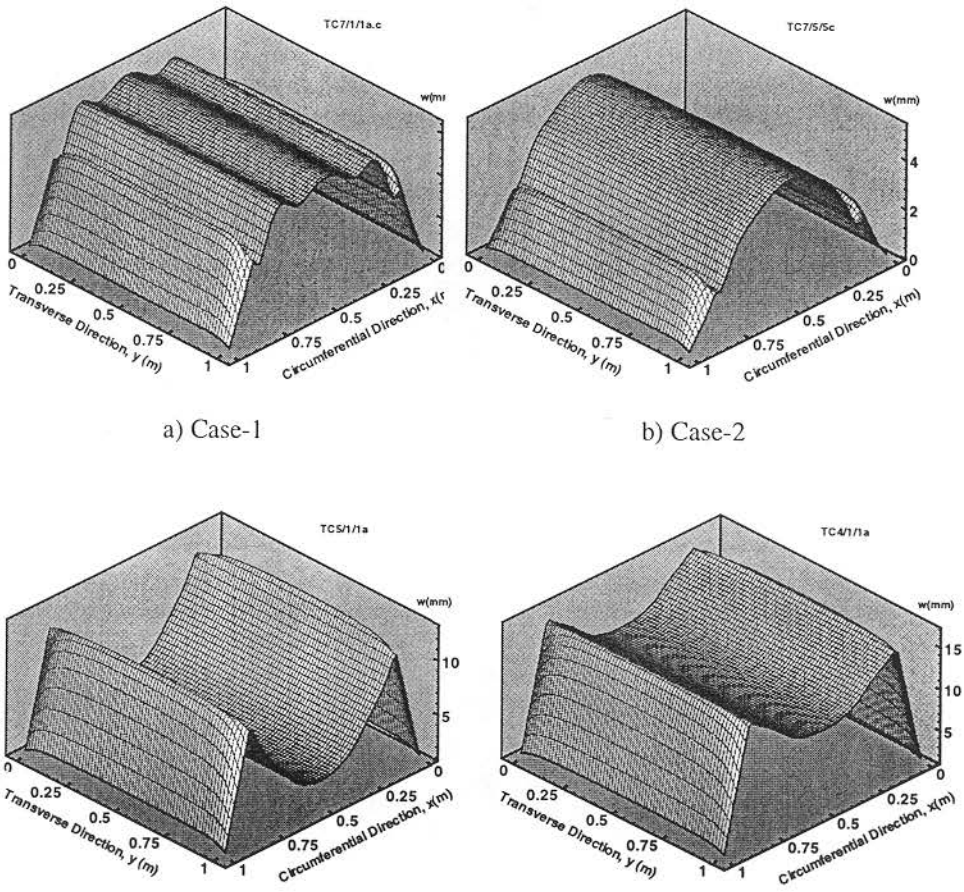

a) Case-1 b) Case-2

c) Case-3 d) Case-4

Figure 5 This figure shows the web-deflections with respect to the initial reference state w_0, for cases-1-4, at steady state, for $p_0 = 600$.

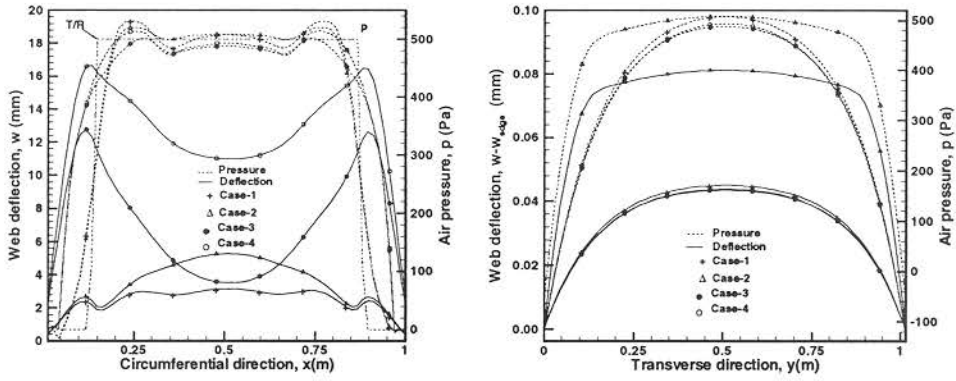

Figure 6 This figure gives a comparison of the mid-line web-deflection, and air pressure distributions for cases-1-4, for the supply pressure of p_0 = 600 Pa. The pull-down pressure distribution, *T/R(x),* is also given.

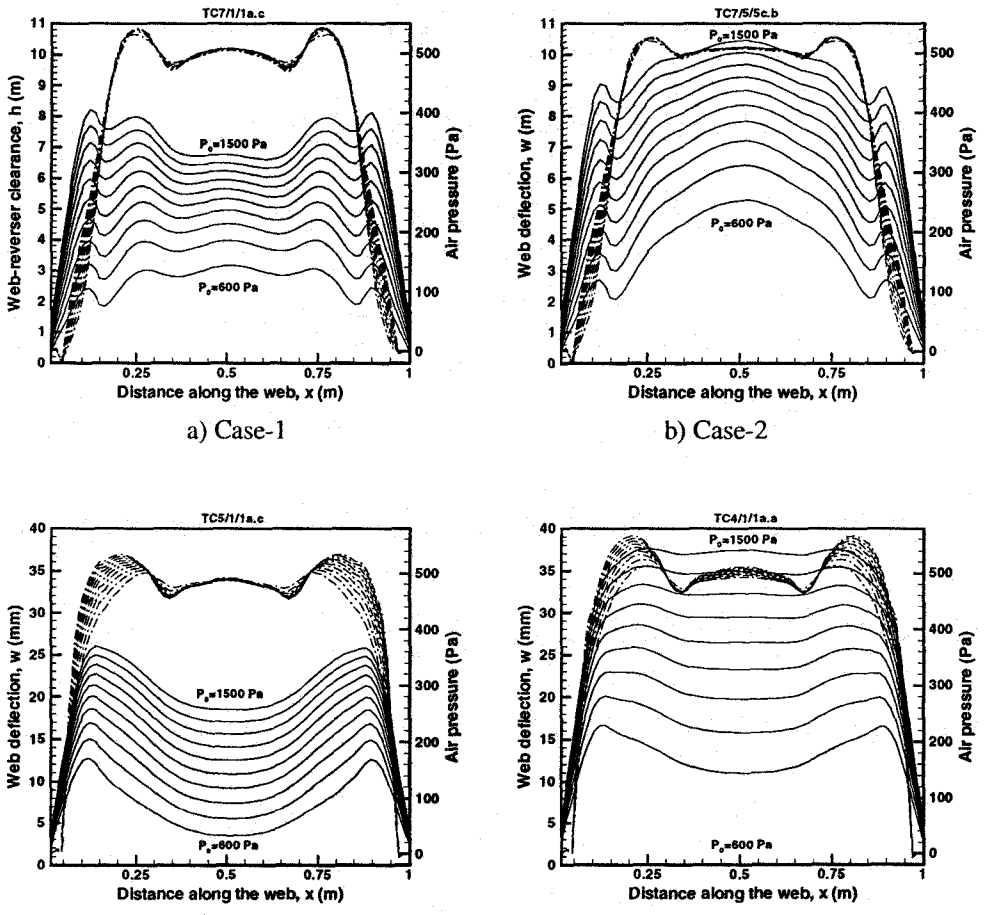

Figure 7 This figure shows the effect of different supply pressures on the steady state web deflection and air pressure distribution, along the center-line of the web.

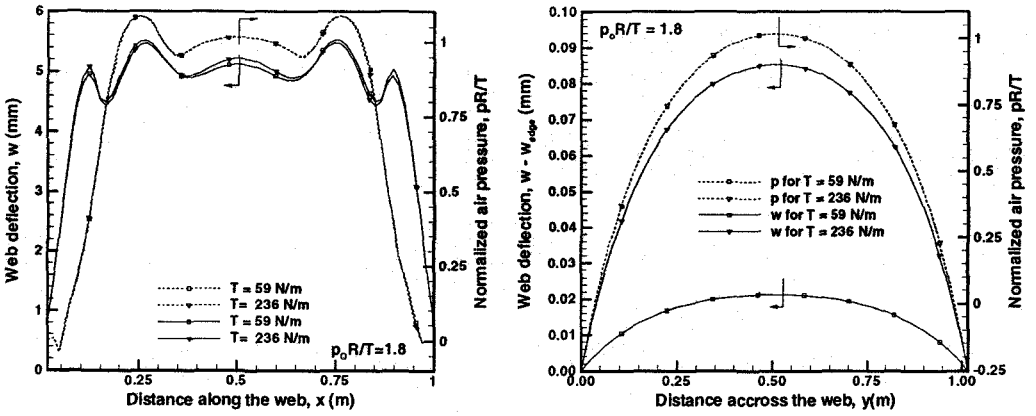

Figure 8 The mid-point $h_{mid} = h(L_x/2,L_y/2)$ and minimum h_{min} web reverser clearance variation with normalized supply pressure p_0R/T.

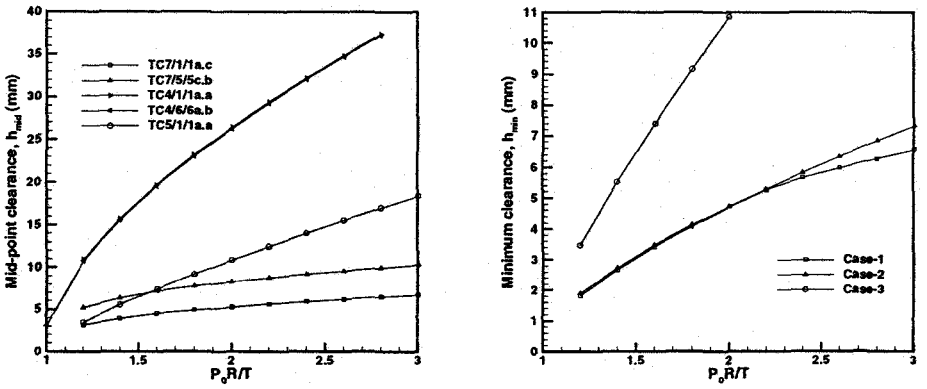

Figure 9 The effect of web tension, T = 59 and 236 N/m, on the web deflection and air pressure at steady state. The normalized supply pressure $p_0R/T = 1.8$ for both cases. This figure shows the cross-sections along midlines $(x,L_y/2)$ and $(L_x/2,y)$.

E	4 GPa
ν	0.3
c	0.2 mm
μ	1.85×10^{-5} Ns/m^2
ρ	1.2 kg/m^3
Web length in each no-wrap region	12.97 cm
Wrap angle	173.44 deg.
R_c	0.25 m
$L_x=L_y$	1.016 m

Table 1 Parameters for the cases presented in this paper.

S. Müftü and K. A. Cole
Mechanics of a Cylindrical Flexible Web Floating Over An Air-Reverser
6/9/99 Session 4 11:30 - 11:55 a.m.

Question - Bob Lucas, Beloit Corporation
You have made the assumption of steady air flow. Many of us with field experience have observed nonsteady, unstable behavior which sometimes leads to noise. Does your analysis have any criteria that would predict the onset of air instability?

Answer - S. Müftü, Massachusetts Institute of Technology
As I've indicated, this is a very complicated two dimensional problem. The current model is first order and does not predict web or air instabilities. However, while not currently planned, such capabilities could be added.

Question - Dave Roisum, Finishing Technologies, Inc.
I've observed that you didn't take advantage of symmetry. Why not?

Answer - S. Müftü, Massachusetts Institute of Technology
We wanted to keep the model general so that such effects as lateral translation and circumferential tension variation could be studied.

Question - Keith Good, Oklahoma State University
From your plot of out-of-plane web deformation, we saw millimeters, which is a lot of deformation. Are you planning an experimental investigation to try to verify these predictions?

Answer - S. Müftü, Massachusetts Institute of Technology
Yes. We need to verify the model. I do want to point out though, that with respect to the self adjusting reference state, the deflections are of order 0.2 millimeters. So, with respect to this reference state, the deflections and curvatures of the web are relatively small and compatible with Donnell's plate theory from which our web deflection equation are derived.

Question - Claude Faulkner, DuPont
One trick used in air reversers is to effect the distribution of air at close clearance points either by creating a dam or by biasing the supply pressure. Are you planning to study these techniques in your work?

Answer - S. Müftü, Massachusetts Institute of Technology
It is possible to use the model to study these effects. I have observed that in the wrap zone that the air pressure tends to be balanced by the belt wrap pressure. Everything else is a function of hole density and hole position. There are obviously infinite possibilities. With help from my sponsors from Kodak and researchers like you, I could get more realistic looking hole densities. Most of the hole densities I've studied to date have been arbitrarily selected and are not necessarily representative of actual design.

Questions - Dave Pfeiffer, JDP Innovations
There are air reversers which use drilled holes and air reversers which use sintered porous metals. Could you compare the two based on your knowledge of that kind of application?

Answer – S. Müftü, Massachusetts Institute of Technology
As I explained, the Reynold's number determines whether air inertia effects or air viscous effects dominate. In some applications, air inertia is not dominant and the air governing equations are different. An example where this is the case will be presented in a paper this afternoon. In these cases, the behavior will be different. Obviously, there is a transition between these two regions. I have not studied the difference between the two. At the limits, however, the behaviors should agree.